DEUTSCHES ELEKTRONEN-SYNCHROTRON DESY

DESY SR-77/01
January 1977

Band Formation in Xenon-Argon Alloys Studied by Photoelectron Spectroscopy

by

R. Nürnberger
II. Institut für Experimentalphysik der Universität Hamburg

F.-J. Himpsel
Sektion Physik der Universität München

E. E. Koch
Deutsches Elektronen-Synchrotron DESY, Hamburg

and

N. Schwentner
Institut für Experimentalphysik der Universität Kiel

2 HAMBURG 52 · NOTKESTIEG 1

Band Formation in Xenon-Argon Alloys Studied by Photoelectron Spectroscopy*

R. Nürnberger

II. Institut für Experimentalphysik der Universität Hamburg, Hamburg

F.-J. Himpsel

Sektion Physik der Universität München, München

E.E. Koch

Deutsches Elektronen-Synchrotron DESY, Hamburg

and

N. Schwentner

Institut für Experimentalphysik der Universität Kiel, Kiel

Photoelectron energy distribution curves for Xenon-Argon alloys for concentrations ranging from 0 - 100 % have been measured by excitation with synchrotron radiation at $h\nu = 13.8$ *eV, 16.5 eV and 18.0 eV. With increasing Xe concentration the gradual formation of Xe valence bands starting from the atomic Xe* $5p_{1/2}$ *and Xe* $5p_{3/2}$ *states is observed. Similarly with Ar the 3p states are broadened with increasing Ar concentration. Rather high concentrations of Xe or Ar are necessary in order to reach the fully developed Xe or Ar bands respectively. The results are discussed in terms of a concentration dependent tightbinding bandstructure.*

---

* Work supported by Deutsches Elektronen-Synchrotron DESY and Bundesministerium für Forschung und Technologie BMFT

I. Introduction

Experimental results for valence states in large band gap insulators e.g. the alkali halides and rare gas solids, have been interpreted in different models which may be crudely classified as (i) local pictures and (ii) band structure models (see e.g. the discussions in Ref. 1 and 2). There is no doubt that the main intrinsic luminescence bands in alkali halides have to be attributed to localized states (such as self trapped excitons) or in the case of rare gas solids to diatomic excimers. The excitonic states leading to the most prominent absorption structures have been treated by ligand field methods in alkali halides whereas they have been attributed to Wannier series in rare gas solids. For the latter case, however, part of the excitonic structure is also observed in liquid rare gases and rare gas-metal mixtures (1,2,3). Surface excitons recently observed in rare gas solids (4) are discussed in terms of disturbed atomic states, taking into account the reduced symmetry at the crystal surface. Further, transport properties like the electron mean free path have been correlated both to the band structure and to atomic ionization cross sections (5). Finally, photoelectron energy distribution curves (PED's) have been compared successfully with band structure calculations (6) implying translational invariance. In particular it has been shown from the angular dependence of photoemission from alkali halides, that the k-vector is a good quantum number (7). From the examples given above it appears that no clear unified picture has emerged so far, and that still more experiments are needed to clarify the situation.

In the present paper we have studied the Xe and Ar valence states by means of photoelectron energy distribution measurements for pure Xe and pure Ar and for mixtures of both with concentrations ranging from 0 - 100 % Xe in Ar. It was recently observed that for small concentrations of Xe guest atoms in an Ar or Ne matrix the Xe states resemble closely the atomic Xe states broadened only by the interaction with the surrounding host matrix (6,8). On the other hand for the pure rare gas solids the experimentally determined valence states have been interpreted by band structure calculations (6). In view of the above mentioned inconsistencies in the description of valence states it seemed worthwile to study experimentally the formation of valence bands as a function of the concentration of guest atoms in a matrix. For the interpretation of our experiments it is essential that in inert gases the guest-host interaction is small compared with the guest-guest interaction. This appears to be reasonable because the guest- and host-states are well separated in energy. Broadening of the valence states in pure rare gas solids by relaxation of the hole state has been proposed very recently as an explanation for the observed bandwidth (9). Predictions for the apparent spin orbit splitting in rare gas mixtures have also been made in Ref. (9). The validity of these ideas can be tested by comparison with the results presented here.

II. Experimental Procedures

The experiments have been performed with synchrotron radiation from the Deutsches Elektronen-Synchrotron (DESY) monochromatized with a normal incidence monochromator at 2 Å resolution. The experimental arrangement, described in detail elsewhere (8,10) allows for combined optical reflection and photoelectron energy distribution measurements at pressures less than 5×10^{-10} Torr. Electrons leaving the sample normal to the surface within a cone of 5° have been analyzed with a resolution of 0.2 eV. The samples have been deposited onto a Helium flow cryostat at temperatures of 8±3 K using gases from L'Air Liquide and Matheson with a purity better than 99.9997 % for Ar and 99.99 % for Xe. The mixtures have been prepared in the gaseous phase with partial pressures according to the desired concentration. The concentration of the deposited samples has been checked by comparison with the integrals of the Xe and Ar contributions to the PED's (Fig. 1). For example, for a mixture of nominal 50 % Xe in Ar a scattering of between 40 % Xe and 60 % Xe has been observed (see errors bars in Fig. 3).

The reflectivity of the samples has been measured between 1500 Å and 8000 Å. A concentration dependence of the reflectivity in the excitonic region very similar to that of Ref. 11 was found. We have tried to identify exciton series for Xe and Ar at all concentrations in order to obtain band gap values for both constituents. However, at higher concentrations no unique assignment was possible.

III. Results and Discussion

Photoelectron energy distribution curves for Xe-Ar mixtures are shown in Fig. 1 for three different photon energies. The position of the maxima in the measured PED's depends on the concentration because both the binding energies of the Xe and Ar valence states with respect to the vacuum level and the band gap are sensitive to the guest-atom concentration. For a clear representation, the energy scale for all PED's in Fig. 1 has been fixed at the maximum due to the Xe $5p_{1/2}$ level (marked by a line in the figure). The positions relative to the vacuum level for the Xe $5p_{1/2}$ level E_V^{Xe} (1/2) and for the top of the Xe-bands E_V^{Xe} and Ar-bands E_V^{Ar} versus the concentration are presented in the upper part of Fig. 2. No background has been subtracted from the experimental PED's in Fig. 1 which have been normalized to the same maximum counting rate. In order to avoid charging of the samples thin films with thicknesses of less than 100 Å have been used. It should be noted that under these conditions hot electrons from the gold substrate can contributed to the PED's (6). Electron-electron scattering is negligible at the low photon energies chosen for the experiments and electron-phonon scattering has only a minor influence (5). The estimated background due to the combined influence of electrons from the gold substrate and secondary electrons is indicated by the dashed lines in Fig. 1.

The PED's represent the joint density of initial and final states but according to our experience for rare gas solids (6,8) the main structures in the PED show the density of initial states to a reasonable approximation. The changes in the PED's from the Xe-states for hν = 13.8 and 18.0 eV surve as an example for the modulation caused by different final states.

The energies involved for the system Xe in Ar have been discussed in detail in Refs. (8,12). The photon energy hν = 13.8 eV is smaller than the binding energy of the Ar bands E_V^{Ar} (with respect to the vacuum level). Thus, only the concentration dependence of the Xe states appears in the first column of Fig. 1. For 5 % Xe in Ar the two maxima correspond to the Xe $5p_{3/2}$ and Xe $5p_{1/2}$ states. This PED is very similar to the PED of 1 % Xe in Ar reported in Ref. (8). In both cases a spin orbit splitting of 1.25 eV is observed. The xperimental halfwidth of $\approx$0.6 eV for the Xe 5p states is a convolution of the experimental resolution of $\approx$0.2 eV with the width of the Xe states in Ar. The latter has to be attributed to the interaction of the Xe atoms with the Ar matrix and with the neighbouring Xe atoms. The Xe-Ar interaction is expected to give only a minor contribution. As a rough estimate we consider the width of exciton bands of $\approx$0.1 eV in absorption spectra for Xe in Ar at low concentrations as discussed by Baldini (13). We conjecture that the dominant contribution to the width is due to broadening by Xe atom pairs. Pair formation occurs already at 5 % Xe with a probability of $\approx$1/2. This influence can be seen also in absorption spectra where the n=1 excitons have a halfwidth of 0.3 eV (11).

The shape and width of the Xe $5p_{1/2}$ structure is rather insensitive to the Xe concentration. For Xe concentration of about 50 % only a small increase in the width is observed and for pure Xe the width is even smaller (see also Fig. 2 $\Delta E^{Xe(1/2)}$). The Xe $5p_{3/2}$ band shows a marked broadening of $\approx$1 eV with increasing Xe concentration. From 5 % Xe to 25 % Xe only a small change in width is observed this being caused by an asymmetric increase at the high energy side of the band. From 20 % Xe to 70 % a second peak appears at the high energy side, which increases even further to a maximum at pure Xe.

Since in the fcc lattice each atom has twelve nearest neighbours, each Xe atom has on the average one other Xe atom at a concentration of about 10 %. Accordingly, the broadening due to Xe pair interaction is almost saturated at 10 % resulting in an observed halfwidth of the Xe $5p_{3/2}$ band of 0.5 to 0.7 eV. This value has to be compared with a width of 1.5 eV at high concentrations. The fact that the width at high Xe concentrations is still increasing, leads to the conclusion that not only the interaction of one Xe pair but that the interaction of three Xe atoms and more determines the features of these bands. For a detailed description, large Xe cluster- or size dependent band structure calculations are needed.

A complete alloying of Xe and Ar is essential for the conclusion drawn above. Such an alloying is supported by optical experiments (14) as well as by the observation of the continuously changing shape of the PED's with changing concentration in the present study.

The behaviour of the Xe band shapes at $h\nu$ = 16.5 and 18 eV is somewhat different from the above because of final state effects. Nevertheless, these spectra reveal also a gradual growth of the Xe bands with increasing concentration.

Electrons from the Ar 3p valence bands are also excited above the vacuum level at the higher photon energies $h\nu$ = 16.5 and 18.0 eV. The concentration dependence is similar to that of the Xe states if one takes into account the smaller

valence bandwidths and the smaller spin orbit splitting of 0.184 eV (4). The half width of the Ar band decreases from E^{Ar} = 1.25 eV for pure Ar to 1.15 eV at 50 % Ar and to 0.7 eV at 10 % Ar in Xe (Fig. 1 and 2). Thus again the major change in band width appears at rather high concentrations of Ar that is between 20 % and 50 %. The half width of $\approx$0.7 eV for 10 % Ar includes both spin-orbit partners and the spin-orbit splitting. The observed width is consistent with a halfwidth of $\approx$0.6 eV of two bands as in the case of Xe separated by a spin orbit splitting of $\approx$0.2 eV which cannot be resolved.

We have made an attempt to describe the concentration dependence of the observed width of the valence bands in terms of a concentration dependent tightbinding band structure. Our results are displayed in Fig. 3. It has been demonstrated for linear chains as an example that with increasing length of the chains there is qualitative agreement for the bandwidth between the results of CNDO and Hartree Fock calculations for molecular orbitals on the one hand and tightbinding band structure calculations on the other hand (see e.g. Ref. 15). For simplicity we have used the band structure approach in the tightbinding scheme (16). The parameters $pp\sigma$, $pp\pi$ and the spin orbit splitting Δ have been determined from the PED of pure Xenon by Rössler (17) to be $pp\sigma = +0.33$; $pp\pi = -0.038$ and $\Delta = 1.37$ eV. The change of $pp\sigma$ and $pp\pi$ with concentration due to the reduced overlap integral of the wave function has been represented by an exponential decrease with increasing mean separation of the Xe atoms using the nearest neighbour distance in solid Xe d_o multiplied by α as a reference length (see Fig. 3). The mean separation has been correlated with the concentration. In Fig. 3 a comparison of the measured valence bandwidth with calculated bandwidths is shown using α as a free parameter. The experimental bandwidth has been determined from the crossing points of the PED's with the dashed lines (Fig. 1) by a linear extrapolation of the PED's at half maximum (see also Fig. 4). For the calculated bandwidth the energy difference between Γ and X has been used because this is the largest width of the bands in the tightbinding approach given the above parameters. For both the Xe and Ar valence states a value of $\alpha = 2$ agrees statisfactorily with the experimentally determined concentration dependence (Fig. 3).

In Fig. 4 the valence bands along the direction from the center of the Brillouin zone Γ to the X point at the boundary are compared with the measured PED's for Xe (upper part) and Ar (lower part) at three concentrations using $\alpha = 2$ for the calculation. The common feature in Fig. 4a for the three photon energies is the appearance of two maxima which correlate quite well with the maxima of the density of states of the lower valence band and of the center of the density of states of the split upper valence bands. The maximum of the density of states is expected to lie at the flat region near the X point. The relative shift of the maxima with reduced Xe concentration is well reproduced by the position of the upper and lower bands at X. Changes in the PED's with photon energy are attributed to structures in the final states. In Fig. 4a such changes are only significant for pure Xe. The splitting of the upper valence band contribution at $h\nu = 13.8$ eV is absent at 50 % Xe/Ar and it disappears entirely at 98% Xe/Ar (Fig. 1) where the total width is practically unaffected. This observation can be taken as a hint that the conduction band states are disturbed by a relatively small concentration of guest atoms.

The similar tendencies found for the Ar valence states (Fig. 4b) support these interpretations but the smaller spin-orbit splitting yields a less clear cut case for the separation of the different contribution. We feel that for Xe and Ar the agreement is encouraging.

A different approach for an understanding of the PED's from rare gas solids and rare gas alloys has been developed recently by Wolff (18). Starting from the assumption that relaxation effects of the surrounding medium lower the local O_h-symmetry of the Ar^+ and Xe^+ ions the splitting of the $3p_{3/2}$ and $5p_{3/2}$ levels due to the removed degeneracy has been calculated. With reasonable ion-medium interaction parameters three p-states are obtained for pure Ar and Xe with splittings close to the experimental observation. It remains to be seen in detail how the alloying changes the interaction parameter and hence the splitting of the states as well as the appearance of the PED's.

Finally we want to discuss the recent paper by Parinello et al. (9) in view of the experimental results presented here. These authors have considered the importance of hole-electron bound states. The considerable difference between the calculated bandwidth for Xe and the bandwidth observed in the PED's (6) has been attributed by Parinello et al. (9) to different relaxation energies of the relaxed holes for the Xe $5p_{3/2}$ and Xe $5p_{1/2}$ valence states. On the basis of a two-band Koster-Slater model the following qualitative predictions for doped rare gas samples have been made (9):

1. For heavy rare gas atoms (Xe) in light rare gas matrices (Ar) no bound state is expected but at higher concentrations of the heavy atoms (Xe) the 3/2 state should shift to higher energies as observed in our experiment.
2. On the other hand a strong bound state is expected for the case of light impurities (Ar) in a matrix of heavy atoms (Xe). Therefore at small Ar concentrations in Xe a large apparent spin orbit splitting is predicted. However, taking a width for the Ar states comparable with that of the Xe states in Ar, a splitting much larger than the real spin-orbit splitting of 0.2 eV does not fit the experimental results.

There are good arguments for interpreting the experimentally determined separation between the top of the Xe $5p_{3/2}$ band and the maximum of the Xe $5p_{1/2}$ structure by considering not only spin-orbit splitting but also by including the width of the lower Xe $5p_{1/2}$ band. Note, that the Xe $5p_{1/2}$ band has its maximum density of states near the boundary of the Brillouin zone. As has been suggested by Rössler [17] the width of this band may be larger than previously assumed because in earlier calculations the constant part of the muffin tin potential had been chosen rather high in order to fit the experimental band gap [19]. With a more realistic potential the valence band width may increase [17] in agreement with the results of other calculations for the ligher rare gas solids.

Acknowledgement

We would like to thank Dr. Lipari for his suggestion that we use the concentration dependent tightbinding approach, Prof. Rössler for the tightbinding model band structure and for stimulating discussions, Dr. E. Tossati for making available to us the manuscript of Ref. 9 prior to publication and H.W. Wolff for stimulating discussions and for making available to us the results of his yet unpublished calculations.

References

1. B. Sonntag, "Dielectric and Optical Properties" in Rare Gas Solids, Eds. M.L. Klein and J.A. Venables, Academic Press 1976, Chapter 17, 1976
2. G. Zimmerer "Optical Excitation and Decay Processes in Rare Gas Solids" in Proceedings of the Intern. Summer School on Synchrotron Radiation Research, Alghero 1976, Ed. I.F. Quercia
3. R.A. Tilton and C.P. Flynn, Phys.Rev.Lett. 34, 20 (1975)
4. V. Saile, M. Skibowski, W. Steinmann, P. Gürtler, E.E. Koch and A. Kozevnikov, Phys.Rev.lett. 37, 305 (1976) and H.-W. Wolff, priv. communication
5. N. Schwentner, Phys.Rev. B15, Dec. 1976
   E.L. Battye, J. Liesegang, R.C.G. Leckey and J.G. Jenkins, Phys.Rev. B13, 2646 (1976)

6a. N. Schwentner, F.-J. Himpsel, V. Saile, M. Skibowski, W. Steinmann and E.E. Koch, Phys.Rev.Lett. 34, 528 (1975)

6b. A.B. Kunz, D.-J. Mickish, S.K.V. Mirmira, T. Shima, F.-J. Himpsel, V. Saile, N. Schwentner and E.E. Koch, Sol. State Comm. 17, 761 (1975); N. Schwentner, F.-J. Himpsel, E.E. Koch, V. Saile and M. Skibowski in: Vacuum Ultraviolet Radiation Physics, Eds: E.E. Koch, R. Haensel and C. Kunz, Pergamon-Vieweg, Braunschweig 1974, p. 355

7. F.-J. Himpsel and W. Steinmann, Phys.Rev.Lett. 35, 1025 (1975) and "Angle resolved Photoemission from the NaCl (100)-face", to be published
8. N. Schwentner and E.E. Koch, Phys.Rev. B14, 4687 (1976)
9. M. Parinello, E. Tosatti, N.H. Mareh and M.P. Tosi, preprint August 1976, to be published
10. N. Schwentner, E.E. Koch, V. Saile, M. Skibowski and A. Harmsen, in: Vacuum Ultraviolet Radiation Physics, Eds: E.E. Koch, R. Haensel and C. Kunz, Pergamon-Vieweg, Braunschweig 1974, p. 792
11. N. Nagasawa, T. Karasawa, N. Miura and T. Nanba, J.Phys.Soc.Jap. 32, 1155 (1972)

12. Z. Ophir, B. Raz, J. Jortner, V. Saile, N. Schwentner, E.E. Koch, M. Skibowski and W. Steinmann, J.Chem.Phys. 62, 650 (1975)

13. C. Baldini, Phys.Rev. 137, 508 (1965)

14. R. Haensel, N. Kosuch, U. Nielsen, U. Rössler and B. Sonntag, Phys.Rev. B7, 1577 (1973)

15. L. Pietronero and N.O. Lipari, J.Chem.Phys. 62, 1796 (1975)

16. J.C. Slater and G.F. Koster, Phys.Rev. 94, 1498 (1954)

17. U. Rössler, private communication

18. H.W. Wolff, private communication

19. U. Rössler, phys.stat.sol. 42, 345 (1970) and "Band Structure and Excitons" in: Rare Gas Solids, Vol. I. Eds.: M.K. Klein and J.A. Venables, Academic Press, Chap. 8, p. 505 (1976)

Figure Captions

Fig. 1 Photoelectron energy distribution curves for Xe/Ar alloys for three different photon energies with the Xe concentration given as a parameter. All spectra are normalized to the same maximum counting rate. The estimated background is indicated by the dashed lines. The energy scale for all PED's has been fixed at the Xe 5p (1/2) maximum. The arrows indicate the onset of photoemission at $E_{kin} = 0$. The dash dotted curve for pure Ar ($h\nu = 18.37$ eV) was taken from Ref. 6a.

Fig. 2 Upper part: Binding energies in eV relative to the vacuum level for the top of the Xe valence bands E_V^{Xe}, the center of the Xe 5p (1/2) level $E_V^{Xe\ 1/2}$ and the top of the Ar valence bands E_V^{Ar} as a function of the Xe concentration. Circles represent data obtained with $h\nu = 13.8$ eV, crosses with $h\nu = 16.5$ eV and triangels with $h\nu = 18.0$ eV respectively.

Lower part: Half widths ΔE in eV for the Xe 5p (3/2), Xe 5p (1/2) and the total Ar 3p valence bands respectively as a function of concentration. The symbols have the same meaning as in the upper part.

Fig. 3 Comparison of the measured total valence band widths in eV for Xe (W_{Xe}) and Ar (W_{Ar}) as a function of concentration including estimated errors (crosses) with calculated band widths. The free parameter α is used in the following expression: $pp\pi(c) = pp\pi(o) \cdot e^{-d/\alpha \cdot d_o}$ and an analogous expression for $pp\sigma$, with (c) and (o) denoting the band structure parameters at a given concentration and for the pure material. d_o is the Xe nearest neighbour distance in pure Xe.

Fig. 4 Comparison of the experimentally determined PED's for Xe at $h\nu = 13.8$, 16.5 and 18.0 eV (upper part) and the Ar valence bands at $h\nu = 16.5$ and 18.0 eV (lower part) for three different concentrations with the calculated valence bands between the Γ and X point using $\alpha = 2$ for the calculation.

DESY 25564

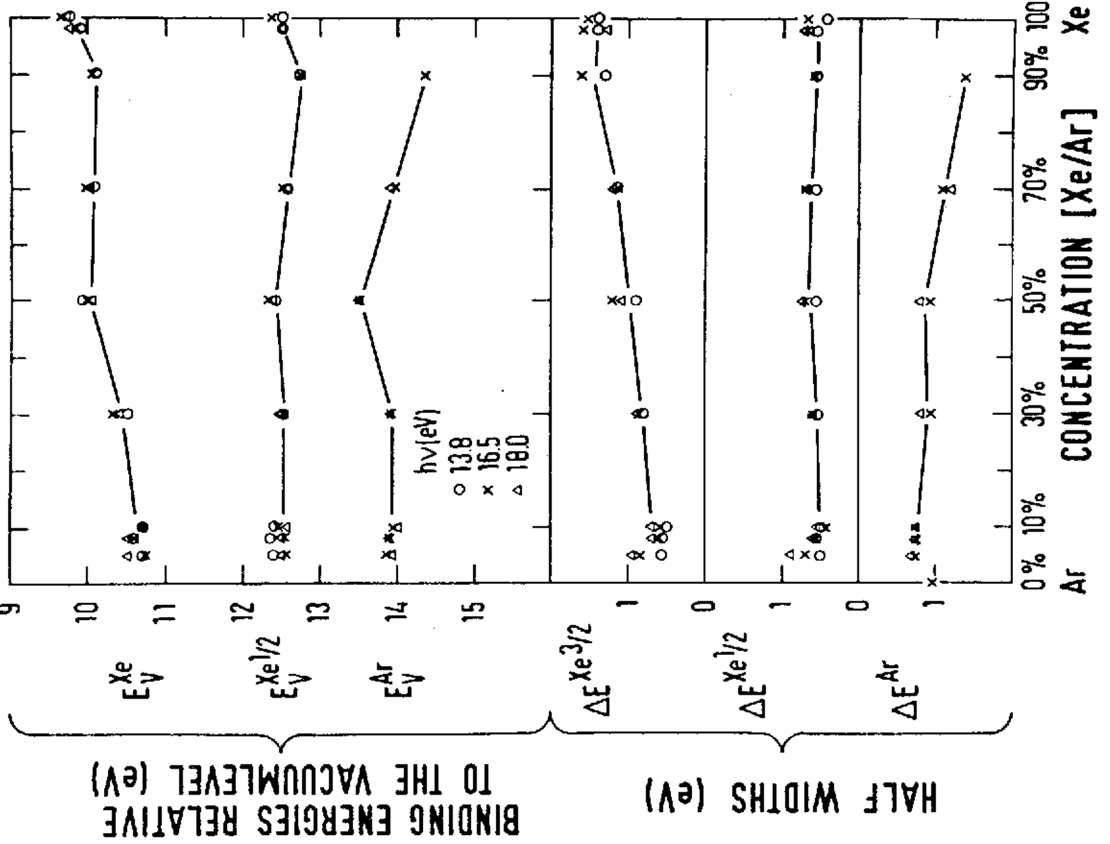

Fig. 2

DESY 25565

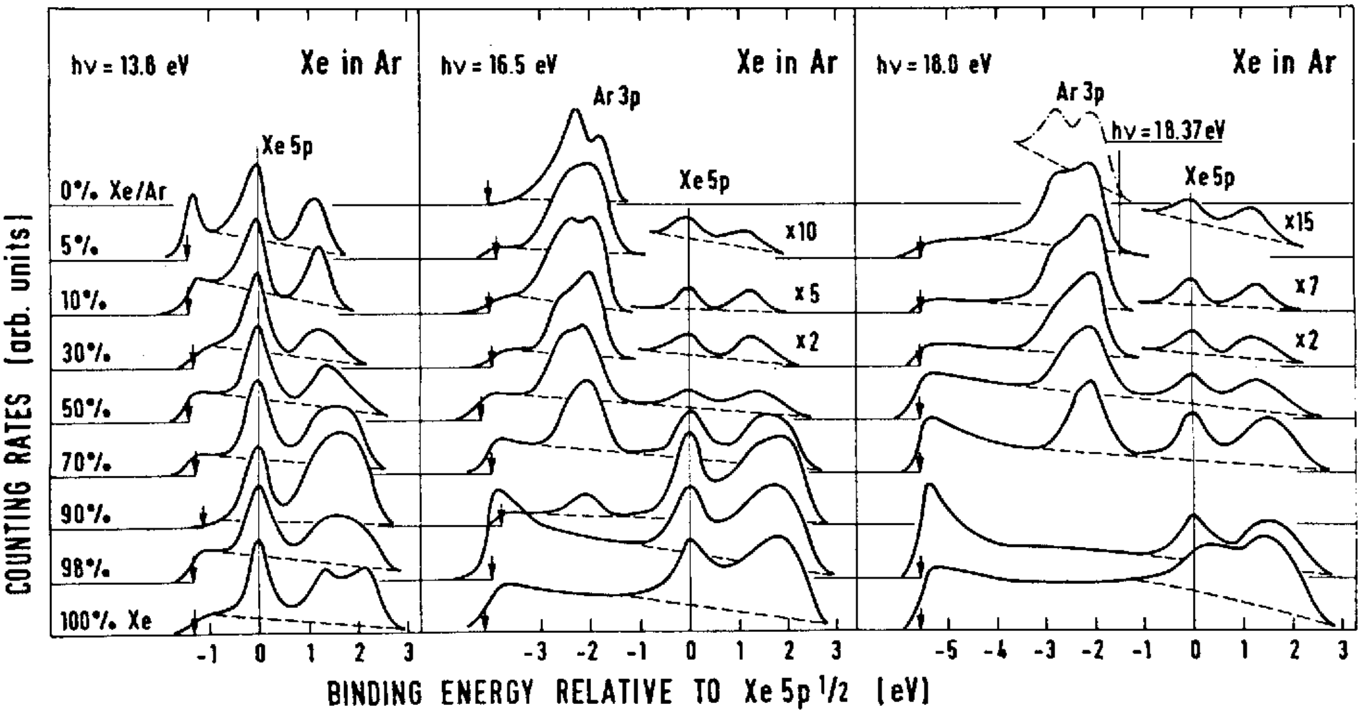

Fig. 1

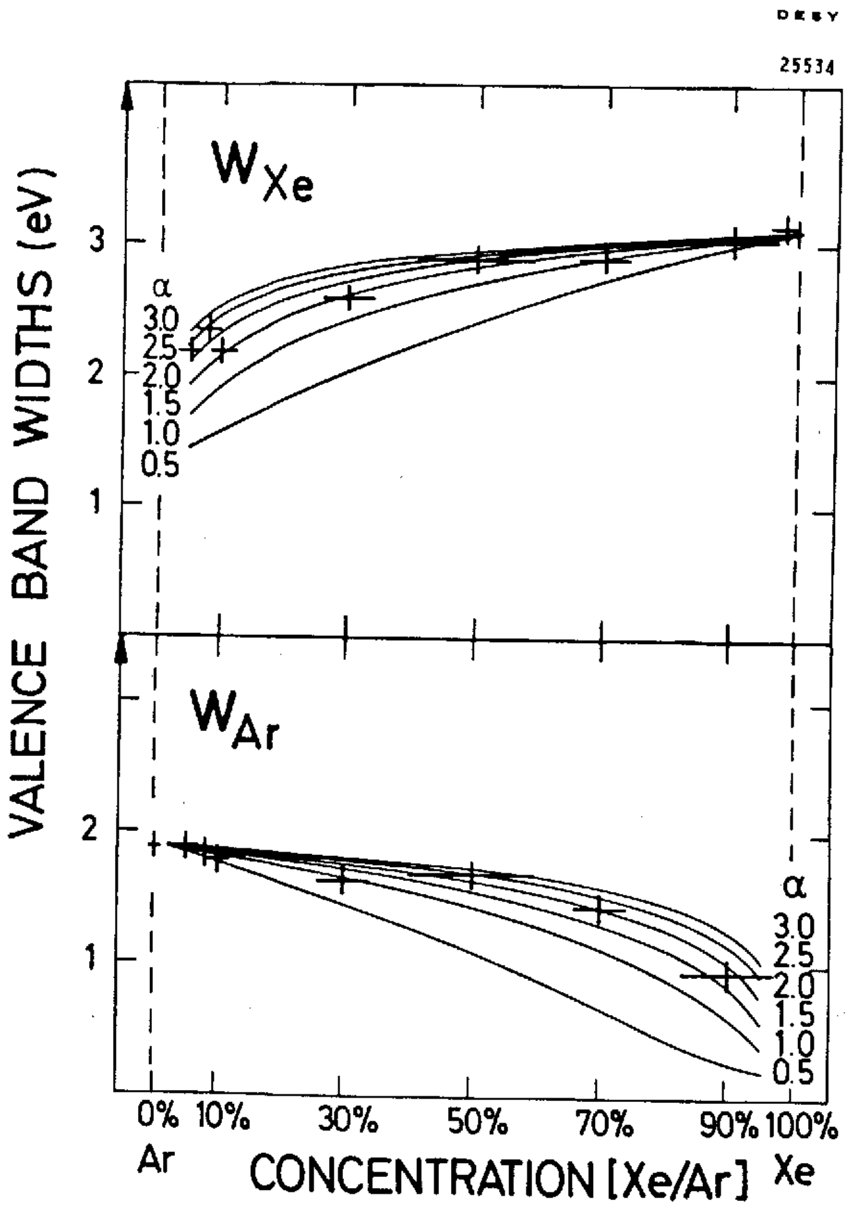
DESY
25534
W_{Xe}
W_{Ar}
VALENCE BAND WIDTHS (eV)
3
2
1
2
1
α
3.0
2.5
2.0
1.5
1.0
0.5
α
3.0
2.5
2.0
1.5
1.0
0.5
0% 10% 30% 50% 70% 90% 100%
Ar
CONCENTRATION [Xe/Ar]
Xe

Fig. 3

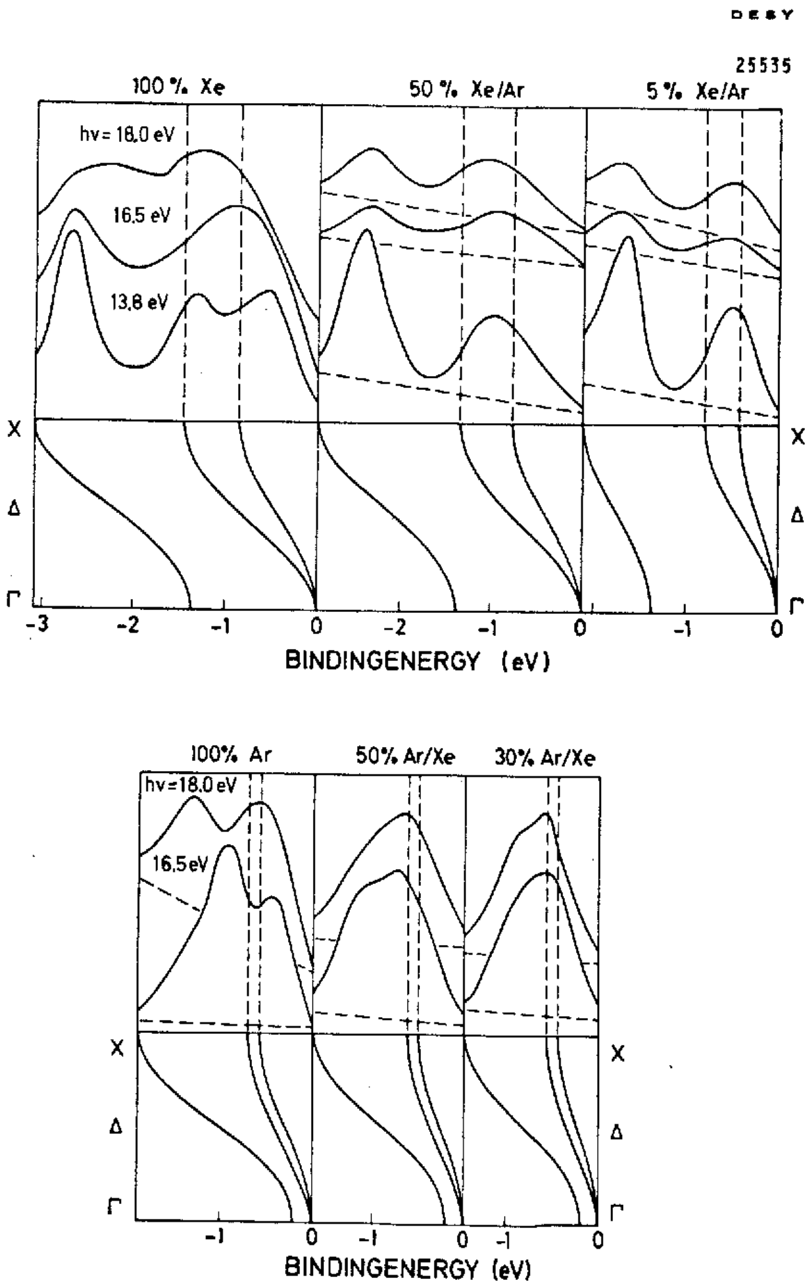
DESY
25535
100 % Xe
50 % Xe/Ar
5 % Xe/Ar
hv= 18.0 eV
16.5 eV
13.8 eV
X
Δ
Γ
-3 -2 -1 0 -2 -1 0 -1 0
BINDINGENERGY (eV)
100% Ar
50% Ar/Xe
30% Ar/Xe
hv=18.0 eV
16.5eV
X
Δ
Γ
-1 0 -1 0 -1 0
BINDINGENERGY (eV)

Fig. 4